Journal of Nuclear Materials 386–388 (2009) 1010–1013

Contents lists available at ScienceDirect

Journal of Nuclear Materials

journal homepage: www.elsevier.com/locate/jnucmat

Clustering of germanium atoms in silica glass responsible for the 3.1 eV emission band studied by optical absorption and X-ray absorption fine structure analysis

Tomoko Yoshida [a,*], Shunsuke Muto [a], Leny Yuliati [b], Hisao Yoshida [b], Yasuhiro Inada [c]

[a] Division of Quantum Science and Energy Engineering, Department of Materials, Physics and Energy Engineering, Nagoya University, Furo-cho, Chikusa-ku, Nagoya 464-8603, Japan
[b] Department of Applied Chemistry, Graduate School of Engineering, Nagoya University, Nagoya 464-8603, Japan
[c] Institute of Materials Structure Science, High Energy Accelerator Research Organization, 1-1 Oho, Tsukuba 305-0801, Japan

A B S T R A C T

Correlation between the 3.1 eV emission band and local atomic configuration was systematically examined for Ge^+ implanted silica glass by UV–vis optical absorption spectroscopy and X-ray absorption fine structure (XAFS) analysis. The 2.7 eV emission band, commonly observed in defective silica, was replaced by the sharp and intense 3.1 eV emission band for the Ge^+ fluence > 2×10^{16} cm^{-2}, in which UV–vis absorption spectra suggested clustering of Ge atoms with the size ~1 nm. XAFS spectroscopy indicated that the Ge atoms were under coordinated with oxygen atoms nearly at a neutral valence state on average. The present results are consistent with the previous ESR study but imply that the small Ge clusters rather than the O=Ge: complexes (point defects) are responsible for the 3.1 eV emission band.

1. Introduction

Silica glass is now widely used as optical windows, insulating parts and optical fibers under fission environments and will be used in future D-T burning fusion apparatus [1–5]. It has been reported that the photosensitivity of silica windows and fibers are closely connected with an absorption band around 5 eV and the corresponding emission band centered at ~3.1 eV [6–9], likely related to Ge impurities. The previous studies, which resorted to photoluminescence (PL), ESR and other spectroscopic techniques, provide important information about the chemical and electronic states of point defects. However, those techniques are insensitive to defects with mesoscopic scale consisting of 10–100 atoms, while the recent sophisticated diffraction techniques only provide a statistically averaged structure.

X-ray absorption fine structure (XAFS) probes the local spatial and electronic structures around a specific element (X-ray absorbing atom), being suitable for the present situation. In addition, a recent state-of-art combination of intense, energy-tunable synchrotron radiation source and a high-sensitive detector has enabled us to obtain a high-quality XAFS spectrum even for an impurity of a very low concentration. In the present study, we successfully obtained the Ge K-edge XAFS of Ge^+-implanted silica glass samples containing Ge as low as ~0.002 at.% within the X-ray probing depth region. The results were compared with the optical properties of the samples to gain insight into what is really responsible for the 3.1 eV emission band.

2. Experimental

The sample used in this study was a synthesized silica glass (T-4040, OH content: 800 ppm) produced by Toshiba Ceramics, Japan, 13 mm in diameter and 2 mm in thickness.

Mass analyzed Ge^+ ions of 30 keV were injected into the samples at room temperature normal to the sample surface. The Ge^+ fluence ranged from 2×10^{14} to 2×10^{16} cm^{-2}. A Monte Carlo calculation (SRIM code) [10] showed that the implanted Ge atoms were distributed up to ca. 50 nm, peaking around 25 nm in depth from the surface.

PL and optical absorption spectra before and after Ge^+ implantation were measured at room temperature using a Hitachi F-4500 spectrometer and a JASCO V-550 optical spectrometer (transmission mode), respectively.

X-ray absorption experiments were carried out at the beam line 9A at Photon Factory in High Energy Accelerator Research Organization Institute of Materials Structure Science at Tsukuba, Japan, using a two-crystal Si(1 1 1) monochromator. A XAFS spectrum of the Ge^+ implanted sample was measured in the fluorescence mode with a high sensitivity 19-element solid-state Ge detector. The X-ray probing depth was estimated to be approximately 0.1 mm from the surface.

* Corresponding author.
E-mail address: tyoshida@nucl.nagoya-u.ac.jp (T. Yoshida).

0022-3115/$ - see front matter © 2009 Published by Elsevier B.V.
doi:10.1016/j.jnucmat.2008.12.201

3. Results and discussion

Fig. 1 shows PL spectra excited by 5 eV light before and after implantation. A weak and broad band is observed before implantation, while the new emission band around 2.7 eV appears after the implantation of 2×10^{15} cm^{-2}. It is likely that the 2.7 eV PL band likely originates from the displacement damages, because a similar PL band was observed in silica irradiated by other ions (H^+, D^+ or He^+) or neutrons [11–14]. The previous studies assigned this PL band to the $B_{2\alpha}$ oxygen deficient centers [6,7] and/or small Si clusters [15].

When the fluence is more than 2×10^{16} cm^{-2}, a sharp and intense 3.1 eV PL band replaces the 2.7 eV band. Cannizzo et al. [16] observed 3.1 eV PL for Ge-doped silica fabricated by a sol–gel method and assigned the PL to a two-fold oxygen-coordinated Ge atom (O=Ge:). On the other hand, Oku et al. [15] claimed that the 3.1 eV PL band from a silica glass containing Ge and GeO_2 nanocrystals was due to the quantum size effect of Ge clusters.

Fig. 2 shows optical absorption spectra of the samples. A large absorption band around 6 eV is seen in the 2×10^{15} cm^{-2} implanted sample. This type of strong absorption peak is commonly seen in metal-implanted silica, suggesting that Ge atoms are atomically dispersed over the entire implanted range [17,18]. In the 2×10^{16} cm^{-2} implanted sample, this large band significantly shrinks suggesting that the isolated Ge atoms begin to produce clusters as the density of implanted Ge increases. Furthermore, the 6 eV band shrinking remains weak, while other broad bands appear at about 4.2 and 5.8 eV. The 5.8 eV band is due to the well known E' band [19], while if we assume that the broad 4.2 eV band is ascribed to small germanium clusters [20], the average cluster size can be estimated by the Mie's resonance scattering formula [21] when the radius, R, of spherical particles is small compared to the wavelength λ of the incident light:

$$R = \frac{V_f \lambda_p^2}{2\pi C \Delta\lambda} \quad (1)$$

where $\Delta\lambda$ is the full-width at half-maximum (FWHM) of the optical absorption peaks, V_f is the Fermi velocity of electrons in bulk metal, C is the speed of light in vacuum, and λ_p is the wavelength of the absorption peak. The average particle size was then estimated to be 1–2 nm.

Fig. 3 shows Ge K-edge XANES spectra of the 2×10^{16} cm^{-2} implanted sample, pure Ge and GeO_2 powder samples. The XANES

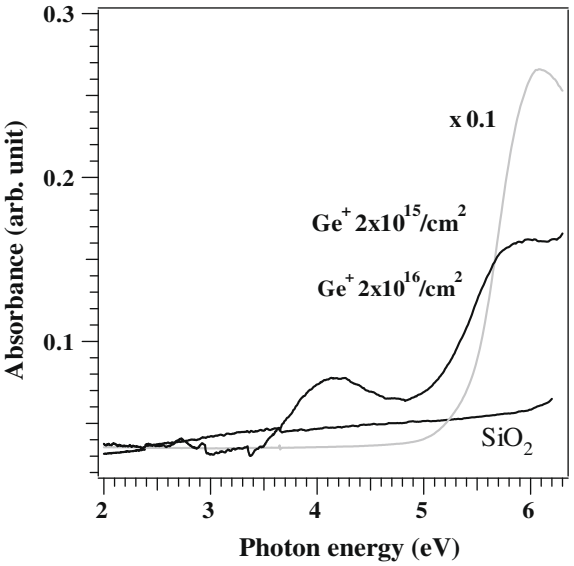

Fig. 2. Optical absorption spectra of silica glass before and after Ge^+ implantation.

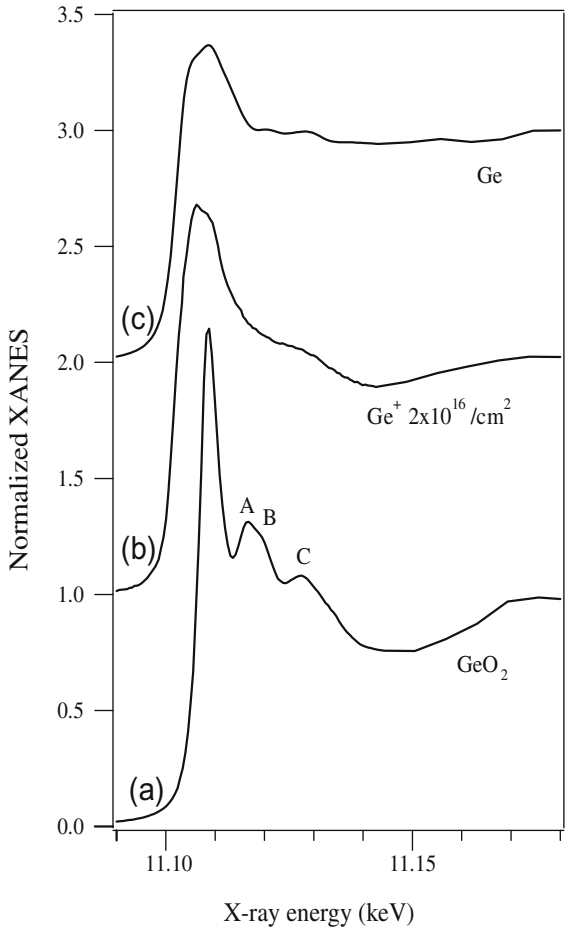

Fig. 3. Ge K-edge XANES spectra from a GeO_2 powder (a), the silica glass implanted with 2×10^{16} Ge^+ cm^{-2} (b) and a Ge powder (c). The peaks A and B are due to the long-range periodic nature of the crystal sample, and the peak C is given rise to by the multiple scattering within the GeO_4 tetrahedron.

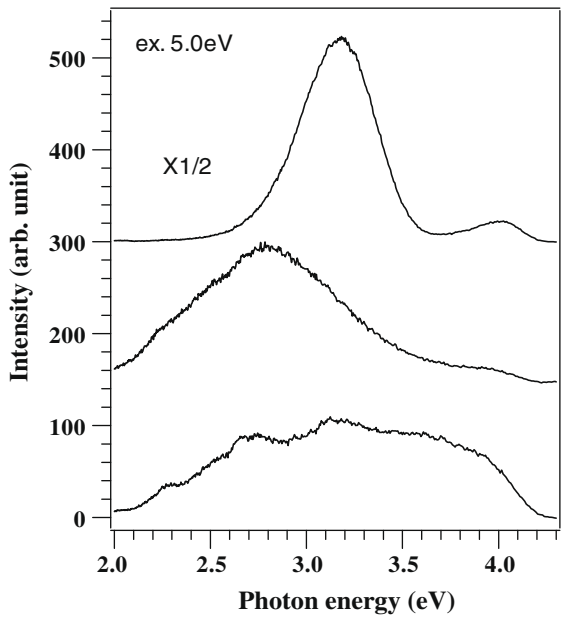

Fig. 1. PL spectra excited by 5 eV light for silica glass before and after Ge^+ implantation.

spectrum of GeO_2 shows characteristic resonance peaks A, B, and C in the post-edge region. It is reported that the peaks A and B are due to the long-range periodic nature of the crystal sample, and the peak C is given rise to by the multiple scattering within the GeO_4 tetrahedron [22,23]. In the XANES spectrum of the implanted sample, the peaks A and B are smeared out while the peak C is still apparent. This feature is similar to that of amorphous GeO_2 and a SiO_2–GeO_2 glass (not shown here) rather than crystalline GeO_2 [23], indicating disordering of the tetrahedral symmetry around Ge. The Ge K-edge threshold of the Ge^+ implanted sample is shifted to the lower energy side by ~4 eV with respect to that of GeO_2, approaching to that of pure Ge. Furthermore, the relative height and width of the first primary peak exhibit a feature between those of Ge and GeO_2. This suggests that each implanted Ge atom takes an intermediate valence state between the neutral (Ge(0)) and tetravalent (Ge(IV)) states. This means that on average Ge atoms are partly bonded to Ge or Si and partly to O.

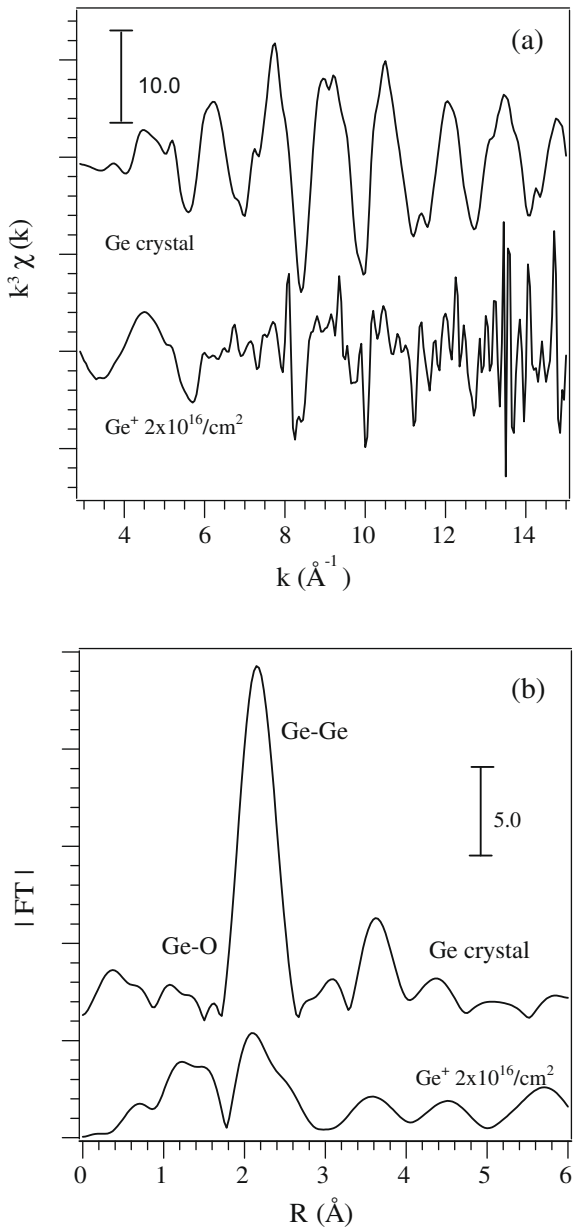

Fig. 4. k^3-weighted Ge K-edge EXAFS spectra of silica glass implanted with 2×10^{16} Ge^+ cm^{-2} and a Ge powder (a), and their radial structural functions (b).

Table 1
Results of curve-fitting analyses.

Sample	Shell	CN	R(Å)	σ(Å)
Ge^+ $2x10^{16}/cm^2$	Ge-O	1.9	1.76	0.09
	Ge-Ge	1.5	2.47	0.0
Ge powder	Ge-Ge	4.0	2.45	0.0

The region of 0.9–2.9 Å in RSFs was inversely Fourier transformed. Theoretical parameters of Ge-O and Ge-Ge shells reported by Mackel were used for curve-fitting. The errors in coordination number and interatomic distance are ± 20% and ± 0.02 Å, respectively. σ is the Debye–Waller factor.

Fig. 4(a) shows k^3-weighted and normalized Ge K-edge EXAFS spectra obtained from the 2×10^{16} cm^{-2} implanted sample and the Ge powder. The main EXAFS oscillation of k = 6–12 $Å^{-1}$ of the Ge^+ implanted sample is similar to, but its amplitude is much smaller than that of the Ge powder. The smaller amplitude of the EXAFS oscillation suggests that a large fraction of Ge atoms are under coordinated, and/or lower symmetry around Ge atoms causes a fast decay of the amplitude. The Fourier transform (FT) of the Ge K-edge EXAFS spectrum in the 3–15.0 $Å^{-1}$ region is shown in Fig. 4(b), as the radial structure function (RSF). At first sight the first peak appearing around 1.5 Å should correspond to the Ge-O bonds and the largest peak observed at 1.8–2.8 Å to the second-neighbour Ge atoms, judging from the peak positions.

To examine the local structure around Ge atoms in further length, we performed nonlinear least-square curve-fitting to the Fourier-filtered EXAFS including the first and the second coordination shells, and the results are summarized in Table 1. In the Ge^+ implanted sample, the Ge-O distance was estimated to be 1.76 Å, which is much longer than the stable Si-O covalent distance, 1.60 Å. The coordination number (CN) of the adjacent oxygen atoms was estimated to be ~2 rather than 4. These results suggest that the implanted Ge atoms are not substituted for the Si site in the SiO_4 unit. On the other hand, the average Ge-Ge distance was estimated to be 2.47 Å, which is in good agreement with that of pure Ge. The average coordination number (CN_{Ge}) for the Ge-Ge shell was estimated to be 1.5, which is significantly smaller than that of pure Ge. Considering that the surface atoms ($CN_{Ge} \leqslant 2$) outnumber the core atoms (germanium $CN_{Ge} \leqslant 4$) for a Ge cluster including less than 100 atoms, these above imply that the size of the small Ge clusters extends no larger than 1 nm, which is quite consistent with the UV absorption results.

4. Conclusion

We examined the local spatial and electronic structures of Ge atoms implanted into silica glass to clarify the origin of the 3.1 emission band by means of optical absorption spectroscopy and XAFS analysis. We concluded that Ge clusters no larger than 1 nm, embedded in the silica glass matrix, are responsible for the 3.1 eV PL band.

Acknowledgement

The present work was supported in part by a Grant-in-Aid for Scientific Research (KAKENHI) in Priority Area (#474) "Atomic Scale Modification" and "Kiban-Kenkyu A" from MEXT, Japan.

References

[1] F.W. Clinard Jr., L.W. Hobbs, in: Physics of Radiation Effects in Crystal, Elsevier, Amsterdam, 1986, p. 442.
[2] R.H. Farnum et al., J. Nucl. Mater. 191–194 (1992) 548.
[3] E.R. Hodgson, J. Nucl. Mater. 191–194 (1992) 552.
[4] E.R. Hodgson, J. Nucl. Mater. 179–181 (1991) 383.
[5] T. Shikama et al., J. Nucl. Mater. 191–194 (1992) 544.

[6] L.N. Skuja, A.N. Streletsky, A.B. Pakovich, Solid State Commun. 50 (1984) 1069.
[7] L.N. Skuja, W. Etzian, Phys. Status Solidi A 96 (1986) 191.
[8] A. Anedda et al., Nucl. Instr. and Meth. B 91 (1994) 405.
[9] A. Anedda, C.M. Carbonaro, R. Corpino, F. Raga, Nucl. Instr. and Meth. B 141 (1998) 719.
[10] <http://www.srim.org/SRIM/SRIM2003.htm>.
[11] T. Ii, T. Yoshida, T. Tanabe, T. Hara, M. Okada, K. Yamaguchi, J. Nucl. Mater. 283–287 (2000) 898.
[12] T. Yoshida, T. Ii, T. Tanabe, H. Yoshida, K. Yamaguchi, J. Nucl. Mater. 307–311 (2002) 1268.
[13] T. Yoshida, T. Tanabe, M. Watanabe, S. Takahara, S. Mizukami, J. Nucl. Mater. 329–333 (2004) 982.
[14] M. Watanabe, T. Yoshida, T. Tanabe, S. Muto, A. Inoue, S. Nagata, Nucl. Instr. and Meth. B 250 (2006) 174.
[15] T. Oku, T. Nakayama, K. Masaki, N. Yasuo, L.R. Wallenberg, K. Niihara, S. Katsuaki, Mater. Sci. Eng. B 74 (2000) 242.
[16] A. Cannizzo, S. Agnello, S. Grandi, M. Leone, A. Magistris, V.A. Radzig, J. Non-Cryst. Solids 351 (2005) 1805.
[17] H. Tsuji, N. Arai, N. Gotoh, T. Minotani, T. Ishibashi, T. Okumine, K. Adachi, H. Kotaki, Y. Gotoh, J. Ishikawa, Surf. and Coat. Tech. 201 (2007) 8516.
[18] K. Shimizu, M. Hashimoto, J. Shibata, T. Hattori, A. Satsuma, Catal. Today 126 (2007) 266.
[19] D.L. Griscom, J. Ceram. Soc. Jpn. 99 (1991) 923.
[20] L. Skuja, K. Kajihara, M. Hirano, A. Saitoh, H. Hosono, J. Non-Cryst. Solids 352 (2006) 2297.
[21] G. Mie, Ann. Phys. 25 (1908) 377.
[22] R.B. Greegor, F.W. Lytke, J. Kortright, A. Fisher-colbrie, J. Non-Cryst. Solids 89 (1987) 311.
[23] O. Majérus, L. Cormier, J.-P. Itie, L. Galoisy, D.R. Neuville, G. Calas, J. Non-Cryst. Solids 345&346 (2004) 34.